Inorg. Chem. **2007**, *46*, 2755–2766

Coordination Studies of a New Unsymmetrical κ^4-PNN′N′′-Tetradentate Ligand: Stepwise Formation and Structural Characterization

Sean E. Durran, Mark R. J. Elsegood, Shelly R. Hammond, and Martin B. Smith*

Department of Chemistry, Loughborough University, Loughborough, Leics, LE11 3TU, U.K.

Received June 30, 2006

The two-step synthesis of a new unsymmetrical ligand 2-{$Ph_2PC_6H_4C(H)$═N}C_6H_4{$N(H)COCH_2N(H)CO_2Bz$}, **2·HH**, via acid-catalyzed Schiff base condensation of 2-(H_2N)C_6H_4{$N(H)COCH_2N(H)CO_2Bz$}, **1**, with 2-$Ph_2PC_6H_4$-(CHO) in refluxing EtOH is reported. The multidentate ligand **2·HH**, isolated in ca. 60% yield, exhibits an array of ligation modes, as exemplified by coordination studies with Ni^{II}, Pd^{II}, Pt^{II}, and Au^{I} mononuclear metal precursors. Hence, reaction of **2·HH** with AuCl(tht) (1:1 molar ratio, tht = tetrahydrothiophene) affords AuCl(**2·HH**), **3**, in which the ligand behaves as a classic, neutral two-electron phosphorus donor. In contrast, reaction with MCl_2(cod) (M = Pt, Pd; cod = cycloocta-1,5-diene) affords the corresponding dichloro complexes MCl_2(**2·HH**) (**4a** M = Pt; **4b** M = Pd) in which κ^2-P/N-chelation through both P and imino N-donor atoms is observed. Likewise, treatment of $Pd(CH_3)Cl$(cod) with **2·HH** gave $Pd(CH_3)Cl$(**2·HH**), **4c**, in which the imino nitrogen is trans to the methyl ligand. Cycloocta-1,5-diene elimination from, and single methyl protonation of, $Pt(CH_3)_2$(cod) with 1 equiv of **2·HH** in toluene at ambient temperature affords the neutral complex $Pt(CH_3)$(**2·H**$^-$), **5a**, in which **2·H**$^-$ functions effectively in a κ^3-PNN′ coordination mode. The dichloro compounds **4a** or **4b** undergo smooth N(H) deprotonation with ^{t}BuOK to give **6a\6a′** and **6b\6b′** in which **2**$^{2-}$ acts as a dianionic κ^4-PNN′N′′ ligand. The corresponding square-planar, diamagnetic, nickel(II) complex **6c\6c′** was prepared in excellent yield from $NiCl_2·6H_2O$, **2·HH**, and ^{t}BuOK. Variable-temperature NMR experiments confirm **6a\6a′** and **6b\6b′** exist, in solution, as a pair of conformational (anti and syn) isomers due to restricted rotation about the N–CO_2Bz group. This feature is also borne out by single-crystal X-ray studies of anti-**6a**·$CHCl_3$, syn-**6a′**·H_2O, anti-**6b**·$CHCl_3$, and anti-**6c**·CH_2Cl_2. To the best of our knowledge, we believe these constitute the first examples of crystallographically characterized conformers of a tetradentate ligand incorporating a P-donor center. All new compounds reported have been fully characterized by a combination of spectroscopic (NMR, FT-IR, ES-MS) and analytical methods. Furthermore, single-crystal X-ray studies have also been undertaken on compounds **2·HH**, **3**, **4a**, and **5a**·Et_2O.

Introduction

There has been increasing interest in the development of new tetradentate ligands, including tetradentate π-radical ligands,[1] with two (or more) different donor centers for their versatile coordination behavior,[2,3] radioimaging/radiotherapeutic uses,[4–6] liquid crystalline,[7] magnetic[8] and phosphorescent properties,[9] and numerous applications in catalysis (including asymmetric synthesis).[10–20] The most popular donor set combinations are those comprising N_2O_2[7,9,21] and

* To whom correspondence should be addressed. E-mail: m.b.smith@lboro.ac.uk. Tel: +44 (0)1509 222553. Fax: +44 (0)1509 223925.

(1) Min, K. S.; Weyhermuller, T.; Bothe, E.; Wieghardt, K. *Inorg. Chem.* **2004**, *43*, 2922−2931.
(2) Costes, J.-P.; Dahan, F.; Donnadieu, B.; Rodriguez Douton, M.-J.; Fernandez Garcia, M.-I.; Bousseksou, A.; Tuchagues, J.-P. *Inorg. Chem.* **2004**, *43*, 2736−2744.
(3) Burger, S.; Therrien, B.; Süss-Fink, G. *Eur. J. Inorg. Chem.* **2003**, 3099−3103.
(4) Visentin, R.; Rossin, R.; Giron, M. C; Dolmella, A.; Bandoli G.; Mazzi, U. *Inorg. Chem.* **2003**, *42*, 950−959.
(5) Jurisson, S. S.; Lydon, J. D. *Chem. Rev.* **1999**, *99*, 2205−2218.
(6) van Bommel, K. J. C.; Verboom, W.; Hulst, R.; Kooijman, H.; Spek, A. L.; Reinhoudt, D. N. *Inorg. Chem.* **2000**, *39*, 4099−4106.
(7) Szydlowska, J.; Krówcyñski, A.; Górecka, E.; Pociecha, D. *Inorg. Chem.* **2000**, *39*, 4879−4885.
(8) Miyasaka, H.; Clérac, R.; Wernsdorfer, W.; Lecren, L.; Bonhomme, C.; Sugiura, K.-I.; Yamashita, M. *Angew. Chem., Int. Ed.* **2004**, *43*, 2801−2805.
(9) Che, C.-M.; Chan, S.-C.; Xiang, H.-F.; Chan, M. C. W.; Liu, Y.; Wang, Y. *Chem. Commun.* **2004,** 1484−1485.
(10) (a) Thomas, C. M.; Mafua, R.; Therrien, B.; Rusanov, E.; Stoeckli-Evans, H.; Süss-Fink, G. *Chem. Eur. J.* **2002**, *8*, 3343−3352. (b) Thomas, C. M.; Süss-Fink, G. *Coord. Chem. Rev.* **2003**, *243*, 125−142.
(11) Trost, B. M.; Van Vranken, D. L.; Bingel, C. *J. Am. Chem. Soc.* **1992**, *114*, 9327−9343.

10.1021/ic061196s CCC: $37.00
Published on Web 03/02/2007

P_2N_2[3,12,15,18,22] atoms although, more recently, examples based on N_2S_2[16,23] have been described. Ourselves[24] and others[25−37] have been interested in terdentate tertiary phosphines of the general type PNX (X = N, P, O, S, or Se donor center). We recently described a new Schiff base ligand and its coordination chemistry with a PNSe donor set combination.[24] Surprisingly, while examples of tetradentate systems of the type P_2N_2 are known, those with P_3N[22d] or PN_3[22a,22b,38,39] combinations are considerably less well documented. This dearth of examples prompted us to seek a simple route to a novel PN_3 tetradentate ligand in which all three N donor centers are different. Herein, we report the synthesis of an unsymmetrical κ^4-PNN′N″-ligand and demonstrate the flexible ligation behavior of this ligand (in its neutral, monoanionic, and dianionic forms) through complexation studies toward linear and square-planar transition metal centers. All compounds have been characterized by multinuclear NMR and FT-IR spectroscopy and in most cases by single-crystal X-ray diffraction studies. We also report here, through a combination of solution NMR and crystallographic studies, the presence of both anti and syn isomers for the tetradentate metal-bound ligand due to hindered N−CO bond rotation.

Experimental Section

Materials. All reactions were carried out in air with the exception of **2·HH** whose synthesis was conducted under an atmosphere of dry, oxygen-free nitrogen using standard Schlenk techniques. All solvents were distilled prior to use. The compounds 2-$(H_2N)C_6H_4$-{N(H)$COCH_2$N(H)CO_2Bz}, **1**,[40] 2-$Ph_2PC_6H_4$(CHO),[41] AuCl(tht) (tht = tetrahydrothiophene),[42] MCl_2(cod) (M = Pt, Pd; cod = cycloocta-1,5-diene),[43] Pd(CH_3)Cl(cod),[44] and Pt$(CH_3)_2$(cod)[45] were prepared according to published procedures. All other reagents were purchased from commercial suppliers and used as received.

Instrumentation. IR spectra were recorded as KBr pellets over the range 4000−200 cm^{-1} using a Perkin-Elmer system 2000 FT spectrometer. ^1H NMR and $^{31}P\{^1H\}$ NMR spectra were recorded either on Bruker AC250 or DPX-400 FT spectrometers with chemical shifts (δ) reported relative to external TMS or H_3PO_4. All NMR spectra (250 or 400 MHz) were recorded in $CDCl_3$ solutions unless otherwise stated. Elemental analyses (Perkin-Elmer 2400 CHN or Exeter Analytical, Inc. CE-440 Elemental Analyzers) were performed by the Loughborough University Analytical Service within the Department of Chemistry. All compounds except **2·HH** were analyzed (Micromass ZQ4000 or Micromass Quattro instruments) by electrospray (ES) in both positive and negative ionization modes using CH_2Cl_2/CH_3OH as the solvent and CH_3OH/H_2O as the liquid flow in which samples were introduced into the source. Compound **2·HH** was analyzed by low-resolution EI and CI (positive ion mode only) using CH_2Cl_2/CH_3OH as the solvent.

(12) Althaus, M.; Bonaccorsi, C.; Mezzetti, A.; Santoro., F. *Organometallics* **2006**, *25*, 3108−3110.
(13) Chen, F.; Feng, X.; Qin, B.; Zhang, G.; Jiang, Y. *Org. Lett.* **2003**, *5*, 949−952.
(14) (a) Wong, W.-K.; Chen, X.-P.; Chik, T.-W.; Wong, W.-Y.; Guo, J.-P.; Lee, F.-W. *Eur. J. Inorg. Chem.* **2003**, 3539−3546. (b) Stoop, R. M.; Mezzetti, A. *Green Chem.* **1999**, *1*, 39−41. (c) End, N.; Macko, L.; Zehnder;, M.; Pfaltz, A. *Chem. Eur. J.* **1998**, *4*, 818−824.
(15) (a) Zhang, H.; Yang, C.-B.; Li, Y.-Y.; Donga, Z.-R.; Gao, J.-X.; Nakamura, H.; Murata, K.; Ikariya, T. *Chem. Commun*. **2003**, 142−143. (b) Gao, J.-X.; Ikariya, T.; Noyori, R. *Organometallics* **1996**, *15*, 1087−1089.
(16) Kim, Y. K.; Livinghouse, T.; Horino, Y. *J. Am. Chem. Soc.* **2003**, *125*, 9560−9561.
(17) Phan, N. T. S.; Brown, D. H.; Adams, H.; Spey, S. E.; Styring, P. *Dalton Trans*., **2004**, 1348 −1357.
(18) Dong, Z.-R.; Li, Y.-Y.; Chen, J.-S.; Li, B.-Z.; Xing, Y.; Gao, J.-X. *Org. Lett.* **2005**, *7*, 1043−1045.
(19) (a) Saito, B.; Katsuki, T. *Angew. Chem., Int. Ed.* **2005**, *44*, 4600−4602. (b) Kang, S. H.; Lee, S. B.; Park, C. M. *J. Am. Chem. Soc.* **2003**, *125*, 15748−15749.
(20) Grutters, M. M. P.; Müller, C.; Vogt, D. *J. Am. Chem. Soc.* **2006**, *128*, 7414−7415.
(21) (a) Hui, J. K.-H.; MacLachlan, M. J. *Chem. Commun*. 2006, 2480−2482. (b) Lam, F.; Xu, J. X.; Chan, K. S. *J. Org. Chem.* **1996**, *61*, 8414−8418.
(22) (a) Dubs, C.; Yamamoto, T.; Inagaki, A.; Akita, M. *Organometallics* **2006**, *25*, 1359−1367. (b) Dubs, C.; Yamamoto, T.; Inagaki, A.; Akita, M. *Organometallics* **2006**, *25*, 1344−1358. (c) Tanaka, S.; Dubs, C.; Inagaki, A.; Akita, M. *Organometallics* **2005**, *24*, 163−184. (d) Hierso, J.-C.; Amardeil, R.; Bentabet, E.; Broussier, R.; Gautheron, B.; Meunier, P.; Kalck, P. *Coord. Chem. Rev*. **2003**, *236*, 143−206. (e) Bennett, J.; Rae, A. D.; Salem, G.; Ward, N. C.; Waring, P.; Wells, K.; Willis, A. C. *J. Chem. Soc., Dalton Trans.* **2002**, 234−243. (f) Liu, X.; Eisenberg, A. H.; Stern, C. L.; Mirkin, C. A. *Inorg. Chem.* **2001**, *40*, 2940−2941. (g) Ligtenbarg, A. G. J.; van den Beuken, E. K.; Meetsma, A.; Veldman, N.; Smeets, W. J. J.; Spek, A. L.; Feringa, B. L. *J. Chem. Soc., Dalton Trans.* **1998**, 263−270. (h) Pilloni, G.; Bandoli, G.; Tisato, F.; Corain, B. *J. Chem. Soc., Chem. Commun.* **1996**, 433−434. (i) Wong, W.-K.; Gao, J.-X.; Wong, W.-T. *Polyhedron* **1993**, *12*, 1047−1053. (j) Cooper, M. K.; Duckworth, P. A.; Hambley, T. W.; Organ, G. J.; Henrick, K.; MacPartlin, M.; Parekh, A. *J. Chem. Soc., Dalton Trans.* **1989**, 1067−1073. (k) Marxen, T. L.; Johnson, B. J.; Nilsson, P. V.; Pignolet, L. H. *Inorg. Chem.* **1984**, *23*, 4663−4670. (l) Jeffery, J. C.; Rauchfuss, T. B.; Tucker, P. A. *Inorg. Chem.* **1980**, *19*, 3306−3316.
(23) Lai, C.-Y.; Mak, W.-L.; Chan, E. Y. Y.; Sau, Y.-K.; Zhang, Q.-F.; Lo, S. M. F.; Williams, I. D.; Leung, W.-H. *Inorg. Chem*. **2003**, *42*, 5863−5870.
(24) Durran, S. E.; Elsegood, M. R. J.; Smith, M. B. *New J. Chem.* **2002**, *26*, 1402−1408.
(25) Hu, W.-Q.; Sun, X.-L.; Wang, C.; Gao, Y.; Tang, Y.; Shi, L.-P.; Xia, W.; Sun, J.; Dai, H.-L.; Li, X.-Q.; Yao, X.-L.; Wang, X.-R. *Organometallics* **2004**, *23*, 1684−1688.
(26) Yang, C.; Cheung, Y. K.; Yao, J.; Wong, Y. T.; Jia, G. *Organometallics* **2001**, *20*, 424−429.
(27) Kniess, T.; Fernandes, C.; Santos, I.; Kraus, W.; Spies, H. *Inorg. Chim. Acta* **2003**, *348*, 237−241.
(28) Dai, H.; Hu, X.; Chen, H.; Bai, C.; Zheng, Z. *Tetrahedron: Asymmetry* **2003**, *14*, 1467−1472.
(29) Britovsek, G. J. P.; Cavell, K. J.; Green, M. J.; Gerhards, F.; Skelton, B. W.; White, A. H. *J. Organomet. Chem*. **1997**, *533*, 201−212.
(30) Correia, J. D. G.; Domingos, A.; Santos, I.; Spies, H. *J. Chem. Soc., Dalton Trans*. **2001**, 2245−2250.
(31) Shi, P.-Y.; Liu, Y.-H.; Peng, S.-M.; Liu, S.-T. *Organometallics* **2002**, *21*, 3203−3207.
(32) van den Beuken, E. K.; Veldman, N.; Smeets, W. J. J.; Spek, A. L.; Feringa, B. L. *Organometallics* **1998**, *17*, 636−644.
(33) Pelagatti, P.; Bacchi, A.; Balordi, M.; Bolaño, S.; Calbiani, F.; Elviri, L.; Gonsalvi, L.; Pelizzi, C.; Peruzzini, M.; Rogolino, D. *Eur. J. Inorg. Chem*. **2006**, 2422−2436.
(34) Boubekeur, L.; Ulmer, S.; Ricard, L.; Mézailles, N.; Le Floch, P. *Organometallics* **2006**, *25*, 315−317.
(35) Bailey, B. C.; Fan, H.; Huffman, J. C.; Baik, M.-H.; Mindiola, D. J. *J. Am. Chem. Soc*. **2006**, *128*, 6798−6799.
(36) Kloek, S. M.; Heinekey, D. M.; Goldberg, K. I. *Organometallics* **2006**, *25*, 3007−3011.
(37) Liang, L.-C. *Coord. Chem. Rev.* **2006**, *250*, 1152−1177.
(38) Watkins, S. E.; Craig, D. C.; Colbran, S. B. *J. Chem. Soc., Dalton Trans*. **2002**, 2423−2436.
(39) Watkins, S. E.; Craig, D. C.; Colbran, S. B. *Inorg. Chim. Acta* **2000**, *307*, 134−138.
(40) Hoyos, O. L.; Bermejo, M. R.; Fondo, M.; García-Deibe, A.; González, A. M.; Maneiro, M.; Pedrido, R. *J. Chem. Soc., Dalton Trans*. **2000**, 3122−3127.
(41) Hoots, J. E.; Rauchfuss, T. B.; Roundhill, D. M. *Inorg. Synth.* **1985**, *21*, 175−179.
(42) Uson, R.; Laguna, A.; Laguna, M. *Inorg. Synth.* **1989**, *26*, 85−91.
(43) (a) Drew, D.; Doyle, J. R. *Inorg. Synth.* **1972**, *13*, 47−55. (b) McDermott, J. X.; White J. F.; Whitesides, G. M. *J. Am. Chem. Soc.* **1976**, *98*, 6521−6528.
(44) Rülke, R. E.; Ernsting, J. M.; Spek, A. L.; Elsevier, C. J.; van Leeuwen, P. W. N. M.; Vrieze, K. *Inorg. Chem*. **1993**, *32*, 5769−5778.
(45) Costa, E.; Pringle, P. G.; Ravetz, M. *Inorg. Synth.* **1997**, *31*, 284−286.

Preparation of 2-{$Ph_2PC_6H_4C(H)$═N}C_6H_4{$N(H)COCH_2N(H)CO_2Bz$} (2·HH). A suspension of **1** (1.001 g, 3.344 mmol), 2-$Ph_2PC_6H_4(CHO)$ (1.001 g, 3.448 mmol), and a catalytic quantity of 4-$CH_3C_6H_4SO_3H$ (0.055 g, 0.289 mmol) in absolute EtOH (50 mL) was refluxed, under a nitrogen atmosphere, for 2 h. After the yellow solution was cooled to room temperature, a yellow solid deposited and was collected by suction filtration. The solid **2·HH** was washed with a small portion of EtOH and dried in vacuo. Yield: 1.164 g (61%). Selected data: ^{31}P ($CDCl_3$): −10.0 ppm. ^{1}H ($CDCl_3$): 9.57 (s, 1H, NH), 8.97 (d, ^{4}J(HP) 3.6, 1H, CH═N), 8.48 (d, ^{3}J(HH) 8, 1H, arom. H), 8.06 (m, 1H, arom. H), 7.45−6.91 (m, 21H, arom. H), 5.61 (br, 1H, NH), 5.15 (s, 2H, OCH_2), 4.20 (d, ^{3}J(HH) 5.6, 2H, NCH_2) ppm. FT-IR (KBr): 3332 (NH), 1721 (CO), 1668 (Amide I), 1538, 1522 (Amide II) cm^{-1}. EI-MS: *m*/*z* 571 [M$^+$]. Anal. Calcd for $C_{35}H_{30}N_3O_3P$: C, 73.54; H, 5.30; N, 7.35. Found: C, 73.38; H, 5.09; N, 7.34.

Preparation of 2-{$Ph_2P(O)C_6H_4C(H)$═N}C_6H_4{$N(H)COCH_2N(H)CO_2Bz$} (2b). Compound **2·HH** (0.103 g, 0.180 mmol) was dissolved in acetone (10 mL), and aqueous H_2O_2 (27.5%, 0.1 mL) was added. The yellow solution was stirred for 80 min and evaporated to dryness under reduced pressure. The solid was redissolved in CH_2Cl_2 (1 mL), and **2b** precipitated by addition of diethyl ether (20 mL) and hexanes (20 mL). The solid was collected by suction filtration and dried in vacuo. Yield: 0.084 g, 79%. Selected data: ^{31}P ($CDCl_3$): 32.3 ppm. ^{1}H ($CDCl_3$): 10.55 (s, 1H, NH), 8.60 (s, 1H, CH═N), 8.46 (d, ^{3}J(HH) 8, 1H, arom. H), 7.97−6.64 (m, 23H, arom. H and NH), 5.09 (s, 2H, OCH_2), 4.33 (d, ^{3}J(HH) 6, 2H, NCH_2) ppm. FT-IR (KBr): 3345, 3230 (NH), 1725 (CO), 1684 (Amide I), 1518 (Amide II), 1176 (PO) cm^{-1}. ES-MS: *m*/*z* 588 [M$^+$]. Anal. Calcd for $C_{35}H_{30}N_3O_4P\cdot0.5H_2O$: C, 70.45; H, 5.25; N, 7.04. Found: C, 70.57; H, 5.23; N, 6.70.

Preparation of AuCl(2·HH) (3). AuCl(tht) (0.0086 g, 0.0268 mmol) and **2·HH** (0.0154 g, 0.0269 mmol) were dissolved in CH_2Cl_2 (0.5 mL) to afford a yellow solution. Diethyl ether was allowed to vapor diffuse into this solution over ca. 14 d to give yellow crystals which were collected by suction filtration and dried in vacuo. Yield: 0.020 g (93%). Selected data: ^{31}P (CD_2Cl_2): 28.8 ppm. ^{1}H (CD_2Cl_2): 8.97 (s, 1H, CH═N), 8.62 (s, 1H, NH), 8.22 (d, ^{3}J(HH) 8.4, 1H, arom. H), 8.16 (s, 1H, arom. H), 7.58−6.86 (m, 21H, arom. H), 6.32 (d, ^{3}J(HH) 8.8, 1H, arom. H), 5.67 (br, 1H, NH), 4.89 (s, 2H, OCH_2), 3.88 (d, ^{3}J(HH) 6, 2H, NCH_2) ppm. FT-IR (KBr): 3331, 3290 (NH), 1722 (CO), 1664 (Amide I), 1536 (sh), 1522 (both Amide II), 330 (AuCl) cm^{-1}. ES-MS: *m*/*z* 768 [M−Cl]. Anal. Calcd. for $C_{35}H_{30}AuClN_3O_3P$: C, 52.28; H, 3.77; N, 5.23. Found: C, 52.39; H, 3.66; N, 5.09.

Preparation of ML_2(2·HH) (M = Pt, L_2 = Cl_2, 4a; M = Pd, L_2 = Cl_2, 4b; M = Pd, L = Cl, CH_3, 4c). $PtCl_2$(cod) (0.064 g, 0.171 mmol) was dissolved in CH_2Cl_2 (20 mL). To this solution **2·HH** (0.099 g, 0.173 mmol) was added to give an immediate orange solution. After the mixture was stirred for 30 min, the volume was reduced under vacuum to ca. 1−2 mL and addition of diethyl ether (30 mL) afforded an orange solid. This was collected by suction filtration and dried in vacuo. Yield: 0.119 g (80%). Compound **4b** was similarly prepared from $PdCl_2$(cod) (98%). Selected data for **4a**: ^{31}P ($CDCl_3$/CH_3OH): 4.2 ppm, ^{1}J(PPt) 3737 Hz. ^{1}H (CD_3SOCD_3): 9.23 (s), 9.19 (s), 8.83 (s), 8.24−6.83 (m, arom. H), 4.99 (s), 4.94 (s), 4.22 (s) ppm. FT-IR (KBr): 3366, 3348 (NH), 1721 (CO), 1685 (Amide I), 1506 (Amide II), 290, 280 (PtCl) cm^{-1}. ES-MS: *m*/*z* 766 [M − 2Cl]. Anal. Calcd for $C_{35}H_{30}Cl_2N_3O_3PPt$: C, 50.18; H, 3.62; N, 5.02. Found: C, 49.91; H, 3.63; N, 4.97. Selected data for **4b** ($CDCl_3$/CH_3OH): ^{31}P: 30.6 ppm. ^{1}H (CD_3SOCD_3): 9.23 (s), 8.59 (s), 8.13 (s), 7.91−6.63 (m, arom. H), 4.97 (s), 3.67 (s) ppm. FT-IR (KBr): 3328 (NH), 1717 (CO), 1681 (Amide I), 1508 (Amide II), 273 (PdCl) cm^{-1}. ES-MS: *m*/*z* 676 [M − 2Cl]. Anal. Calcd for $C_{35}H_{30}Cl_2N_3O_3PPd\cdot0.25OEt_2$: C, 52.53; H, 3.99; N, 5.11. Found: C, 52.78; H, 4.20; N, 4.70. Compound **4c** was similarly prepared from **2·HH** and Pd(CH_3)Cl(cod) in 92% yield. Selected data for **4c**: ^{31}P ($CDCl_3$): 36.9 ppm. ^{1}H ($CDCl_3$): 8.90 (s, 1H, CH═N), 8.07 (s, 1H, NH), 7.58−7.01 (m, 22H, arom. H), 6.14 (d, ^{3}J(HH) 7.5, 1H, arom. H), 5.44 (s, 1H, NH), 4.89 (s, 2H, OCH_2), 3.85 (d, ^{3}J(HH) 5.6, 2H, NCH_2), 0.60 (d, ^{3}J(HP) 3.1, 3H, $PdCH_3$) ppm. FT-IR (KBr): 3346, 3330 (NH), 1722 (CO), 1682 (Amide I), 1508 (Amide II) cm^{-1}. ES-MS: *m*/*z* 714 [M − CH_3]. Anal. Calcd for $C_{36}H_{33}ClN_3O_3PPd$: C, 59.35; H, 4.57; N, 5.77. Found: C, 59.13; H, 4.46; N, 5.58.

Preparation of MCH_3(2·H) (M = Pt, 5a; M = Pd, 5b). Pt(CH_3)$_2$(cod) (0.019 g, 0.057 mmol) and **2·HH** (0.032 g, 0.056 mmol) were dissolved in toluene (1 mL) to afford an orange solution. After ca. 2 h, a yellow solid formed and this mixture was left to stand for a further 2 days. The solid was collected by suction filtration and dried in vacuo. Yield: 0.036 g (81%). Selected data for **5a**: ^{31}P ($CDCl_3$): 15.9 ppm, ^{1}J(PPt) 3865 Hz. ^{1}H ($CDCl_3$): 8.65 (m, ^{3}J(HPt) 39.7, 1H, CH═N), 8.14 (d, ^{3}J(HH) 8.3, 1H, arom. H), 7.52−6.84 (m, 22 H, arom. H), 5.90 (s, 1H, NH), 5.09 (s, 2H, OCH_2), 4.29 (d, ^{3}J(HH) 4.3, 2H, NCH_2), 0.69 (m, ^{2}J(HPt) 85.8 Hz, 3H, $PtCH_3$) ppm. FT-IR (KBr): 3302 (NH), 1712 (CO), 1616 (Amide I) cm^{-1}. ES-MS: *m*/*z* 781 [M$^+$]. Anal. Calcd for $C_{36}H_{32}N_3O_3PPt$: C, 55.45; H, 4.02; N, 5.39. Found: C, 55.60; H, 4.05; N, 5.22. Compound **5b** was prepared in 96% from **4c** and ^{t}BuOK in CH_3OH. Selected data for **5b**: ^{31}P ($CDCl_3$): 39.8 ppm. ^{1}H ($CDCl_3$): 8.33 (s, 1H, CH═N), 8.02 (d, ^{3}J(HH) 8.3, 1H, arom. H), 7.59−6.72 (m, 22 H, arom. H), 5.92 (s, 1H, NH), 5.05 (s, 2H, OCH_2), 4.15 (d, ^{3}J(HH) 4.2, 2H, NCH_2), 0.39 (d, ^{3}J(HP) 3.7 Hz, 3H, $PdCH_3$) ppm. FT-IR (KBr): 3287 (NH), 1724 (sh), 1710 (both CO), 1592 (Amide I) cm^{-1}. ES-MS: *m*/*z* 692 [M$^+$]. Anal. Calcd for $C_{36}H_{32}N_3O_3PPd$: C, 62.47; H, 4.67; N, 6.07. Found: C, 62.32; H, 4.58; N, 6.11.

Preparation of M(2) (M = Pt, anti-6a\syn-6a′; M = Pd, anti-6b\syn-6b′). Method 1. A CH_3OH (15 mL) solution of **4a** (0.052 g, 0.062 mmol) and ^{t}BuOK (0.029 g, 0.258 mmol) were refluxed for 3 h. The orange solution was cooled and evaporated to dryness. The residue was extracted into CH_2Cl_2 (25 mL) and passed through a small Celite plug, and the volume concentrated under reduced pressure to ca. 1−2 mL. Addition of diethyl ether (10 mL) and petroleum ether (bp 60−80 °C, 10 mL) gave anti-**6a**\syn-**6a′**. Yield: 0.047 g (97%). Compound anti-**6b**\syn-**6b′** was similarly prepared from **4b** (75%). Selected data for anti-**6a**\syn-**6a′**: ^{31}P ($CDCl_3$, 295 K): 12.3, 12.0 ppm, ^{1}J(PPt) 3492, 3508 Hz (ca. 1:1 ratio). ^{1}H ($CDCl_3$, 295 K): 8.95−8.53 (m, arom. H), 7.96−6.90 (m, arom. H), 4.80 (s), 4.70 (s), 4.66 (s), 3.90 (s) (all CH_2) ppm. ^{1}H ($CDCl_3$, 333 K): 8.87 (d, ^{3}J(HH) 8.4, 1H, arom. H), 8.82 (m,^{3}-(HPt) 80, 1H, CH═N), 8.14−6.89 (m, 22H, arom. H), 4.70 (m, ^{3}J(HPt) 27.2, 2H, NCH_2), 4.52 (br, 2H, OCH_2). FT-IR (KBr): 1656 (CO), 1624 (Amide I) cm^{-1}. ES-MS: *m*/*z* 765 [M$^+$]. Anal. Calcd for $C_{35}H_{28}N_3O_3PPt\cdot H_2O$: C, 53.71; H, 3.87; N, 5.37. Found: C, 53.30; H, 3.71; N, 5.32. Selected data for anti-**6b**\syn-**6b′**: ^{31}P ($CDCl_3$, 295 K): 26.5, 26.3 ppm (ca. 1:1 ratio). ^{1}H ($CDCl_3$, 295 K): 8.60−8.43 (m, arom. H), 7.86−6.79 (m, arom. H), 4.61 (s), 4.55 (s), 3.85 (s) (all CH_2) ppm. ^{1}H ($CDCl_3$, 333 K): 8.67 (d, ^{3}J-(HH) 7.6, 1H, arom. H), 8.53 (s, 1H, CH═N), 7.84−6.81 (m, 22H, arom. H), 4.55 (s, 2H, NCH_2), 4.38 (br, 2H, OCH_2). FT-IR (KBr): 1640 (CO), 1614 (Amide I) cm^{-1}. ES-MS: *m*/*z* 676 [M$^+$]. Anal. Calcd for $C_{35}H_{28}N_3O_3PPd$: C, 62.18; H, 4.18; N, 6.22. Found: C, 61.75; H, 3.96; N, 6.18.

Method 2. To an orange CH_2Cl_2 (7 mL) solution of Pd(OAc)$_2$ (0.043 g, 0.192 mmol) was added **2·HH** (0.110 g, 0.192 mmol).

Table 1. Details of the X-ray Data Collections and Refinements for Compounds **2·HH**, **3**, **4a**, **5a**·Et_2O, anti-**6a**·$CHCl_3$, syn-**6a**′·H_2O, anti-**6b**·$CHCl_3$, and anti-**6c**′·CH_2Cl_2

compound	**2·HH**	**3**	**4a**	**5a**·Et_2O	anti-**6a**·$CHCl_3$	syn-**6a**′·H_2O	anti-**6b**·$CHCl_3$	anti-**6c**′·H_2Cl_2
formula	$C_{35}H_{30}N_3O_3P$	$C_{35}H_{30}AuClN_3O_3P$	$C_{35}H_{30}Cl_2N_3O_3PPt$	$C_{40}H_{42}N_3O_4PPt$	$C_{36}H_{29}Cl_3N_3O_3PPt$	$C_{35}H_{30}N_3O_4PPt$	$C_{36}H_{29}Cl_3N_3O_3PPd$	$C_{36}H_{30}Cl_2NiN_3O_3P$
M	571.59	804.01	837.58	854.83	884.03	782.68	795.34	713.21
cryst dimens, mm^3	0.33 × 0.22 × 0.10	0.28 × 0.22 × 0.03	0.24 × 0.15 × 0.10	0.41 × 0.22 × 0.16	0.18 × 0.16 × 0.02	0.25 × 0.20 × 0.09	0.27 × 0.23 × 0.05	0.47 × 0.26 × 0.04
cryst morphology and color	block, yellow	plate, yellow	block, yellow	block, orange	plate, orange	block, orange	plate, orange	plate, red
cryst syst	triclinic	orthorhombic	triclinic	monoclinic	triclinic	monoclinic	triclinic	triclinic
space group	$P\bar{1}$	*Pcca*$_1$	$P\bar{1}$	$P2_1$	$P\bar{1}$	$P2_1/c$	$P\bar{1}$	$P\bar{1}$
a/Å	5.7163(4)	10.2646(3)	10.2631(4)	10.9918(4)	12.1259(6)	10.5410(7)	12.1068(6)	11.8195(5)
b/Å	14.0540(9)	24.5437(8)	12.6371(5)	20.1329(8)	12.3708(6)	12.7066(9)	12.4003(6)	12.3734(5)
c/Å	18.9410(12)	25.2894(8)	13.9101(5)	16.9331(6)	12.7204(6)	22.8534(16)	12.6708(6)	12.4974(5)
α/(deg)	102.739(2)		108.757(2)		88.533(2)		88.378(2)	89.552(2)
β/(deg)	91.825(2)		107.033(2)	101.717(2)	86.397(2)	94.996(2)	86.176(2)	65.190(2)
γ/(deg)	93.739(2)		90.723(2)		63.724(2)		63.823(2)	85.840(2)
V/Å^3	1479.37(17)	6371.2(3)	1621.93(11)	3669.2(2)	1707.60(14)	3049.4(4)	1703.34(14)	1654.14(12)
Z	2	8	2	4	2	4	2	2
μ/mm^{-1}	0.134	4.792	4.580	3.912	4.431	4.699	0.868	0.837
θ range/°	1.64−29.01	0.83−27.50	1.71−29.01	1.59−29.10	1.60−28.97	1.79−28.89	1.83−29.07	1.80−29.21
measured reflns	13 267	52 953	14 573	30 665	15 289	22 959	15 299	14 977
independent reflns	6873	14 442	7543	16 450	7903	7304	7929	7768
observed reflns ($F^2 > 2\sigma(F^2)$)	5213	11 414	6999	14 266	7026	5921	6898	6405
R_{int}	0.0160	0.0473	0.0137	0.0261	0.0238	0.0251	0.0157	0.0179
$R1$ [$F^2 > 2\sigma(F^2)$][a]	0.0399	0.0368	0.0173	0.0282	0.0262	0.0215	0.0311	0.0378
$wR2$ [all data][b]	0.1035	0.0773	0.0390	0.0503	0.0612	0.0449	0.0776	0.1000
largest difference map features/eÅ^3	0.355, −0.287	1.856, −1.421	0.660, −0.504	1.539, −0.851	1.332, −1.319	0.712, −0.592	0.757, −1.075	0.929, −0.802

[a] $R1 = \sum||F_o| - |F_c||/\sum|F_o|$. [b] $wR2 = [\sum[w(F_o^2 - F_c^2)^2]/\sum[w(F_o^2)^2]]^{1/2}$.

Figure 1. ORTEP plot of ligand **2·HH** showing the bifurcated intramolecular H-bonding. Thermal ellipsoids are drawn at the 50% probability level.

An instant deep red solution formed, which was stirred at ambient temperature for 1 h. The volume was concentrated under reduced pressure to ca. 1−2 mL and Et_2O (20 mL) added. The solid anti-**6b**\syn-**6b′** was collected by suction filtration and dried in vacuo. Yield: 0.120 g (93%).

Preparation of Ni(2) (anti-6c\syn-6c′). A CH_3OH (10 mL) solution of $NiCl_2 \cdot 6H_2O$ (0.031 g, 0.130 mmol), **2·HH** (0.076 g, 0.133 mmol), and ^{t}BuOK (0.039 g, 0.348 mmol) was refluxed for 1 h. The deep red solution was cooled and the volume concentrated to ca. 2−3 mL to afford a bright orange solid. The solid was collected by suction filtration, washed with a small portion of CH_3OH, and dried in vacuo. Yield: 0.067 g (82%). Selected data for anti-**6c**\syn-**6c′**: ^{31}P ($CDCl_3$, 295 K): 20.3, 19.2 ppm (ca. 1:3 ratio). ^{1}H ($CDCl_3$, 295 K): 8.42−6.79 (m, arom. H and CH═N), 4.39, 4.09, 3.84 (CH_2) ppm. FT-IR (KBr): 1630 (CO), 1617 (sh, Amide I) cm^{-1}. ES-MS: *m*/*z* 628 [M^+]. Anal. Calcd for $C_{35}H_{28}N_3O_3PNi$: C, 66.90; H, 4.50; N, 6.69. Found: C, 66.75; H, 4.21; N, 6.79.

X-ray crystallography. Suitable crystals were grown by vapor diffusion of diethyl ether into either a CH_2Cl_2 (for **3** and anti-**6c**) or $CDCl_3$ (for **5a**, anti-**6a**, and anti-**6b**) solution. Approximately 3 mg of X-ray quality crystals of syn-**6a′** were obtained by allowing a methanol solution of **4a**/^{t}BuOK to stand overnight. Slow evaporation of a CH_2Cl_2/Et_2O filtrate (for **4a**) or solution (for **2·HH**) afforded suitable X-ray quality crystals. All measurements were made on a Bruker AXS SMART 1000 CCD area-detector diffractometer, at 150 K, using graphite-monochromated Mo K_α radiation (λ = 0.71073 Å) and narrow frame exposures (0.3°) in ω. Cell parameters were refined from the observed (ω) angles of all strong reflections in each data set. Intensities were corrected semiempirically for absorption based on symmetry-equivalent and repeated reflections. The structures were solved by direct methods (Patterson synthesis for anti-**6b** and anti-**6a**) and refined on F^2 values for all unique data by full-matrix least-squares. Table 1 gives further details. All non-hydrogen atoms were refined anisotropically. Programs used were Bruker AXS SMART and SAINT for diffractometer control and frame integration,[46] Bruker SHELXTL for structure solution, refinement and molecular graphics,[47] and local programs.

For **2·HH**, the atoms C(25)−C(29) are disordered over two sets of positions with C(24) common to both disorder components. This disorder was refined with restraints on geometry and anisotropic

(46) *SMART and SAINT software for CCD diffractometers*; Bruker AXS Inc.: Madison, WI, 2001.
(47) Sheldrick, G. M. *SHELXTL user manual, version 6.10*; Bruker AXS Inc.: Madison, WI, 2000.

Scheme 1. Preparation of **2·HH**[a]

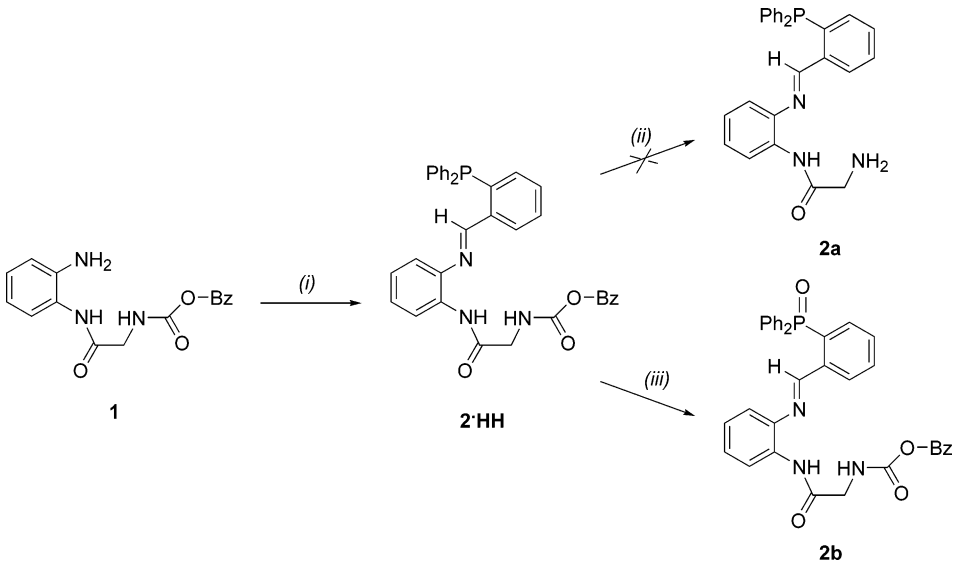

[a] Key: Reagents and conditions: (*i*) 2-$Ph_2PC_6H_4$(CHO), H^+, EtOH, reflux, 2 h (*ii*) 10% Pd/C, cyclohexene, EtOH, reflux, 2 h (*iii*) aq H_2O_2 (27.5%), $(CH_3)_2CO$.

displacement parameters. Major/minor components = 53.1:46.9(4)%. N*H* hydrogens had coordinates freely refined, C*H* hydrogens were included in a riding model. For **4a**, the atoms O(3), C(17), and C(19)−C(23) are split over two sets of positions and were refined as above. Major/minor components = 69.8:30.2(6)%. Absolute structure parameters for **3** (twinned by inversion) and **5a**·Et_2O were 0.512(5) and −0.009(4), respectively. Structures anti-**6a**·$CHCl_3$ and anti-**6b**·$CHCl_3$ are isostructural. In anti-**6c**·CH_2Cl_2, the metal complex is essentially isostructural with anti-**6a** and anti-**6b**, but due to the different solvent of crystallization, it is not isomorphous with anti-**6a**·$CHCl_3$ and anti-**6b**·$CHCl_3$.

Results and Discussion

Ligand Synthesis. Our synthesis of the new κ^4-PNN′N″ tetradentate ligand, **2·HH**, was accomplished in two steps starting from 1,2-diaminobenzene. Using a known procedure, reaction of 1,2-diaminobenzene with carbobenzyloxyglycine and dicyclohexylcarbodiimide in THF gave **1** (Scheme 1) in 78%.[40] The availability of the primary amine group in **1** allows for introduction of the two remaining donor atoms (imine N and $-PPh_2$ moieties). The aldehyde-phosphine 2-$Ph_2PC_6H_4$(CHO) has previously been shown to be an extremely useful building block for the synthesis of multifunctional ligands by a classic Schiff base condensation.[20,26,38,39,48] Our initial attempt to condense **1** with 2-$Ph_2PC_6H_4$(CHO) in refluxing absolute ethanol for 48 h gave **2·HH**, albeit in very low yield (20%). Analysis of the reaction mixture by $^{31}P\{^1H\}$ NMR spectroscopy revealed a significant amount of unreacted 2-$Ph_2PC_6H_4$(CHO). We found the yield of **2·HH** could be significantly increased to 61% and reflux time reduced to 2 h by addition of a small quantity of 4-$CH_3C_6H_4SO_3H$ as an acid catalyst.[49] No further attempts were made to optimize this yield which is comparable to previous dehydration reactions using 2-$Ph_2PC_6H_4$(CHO) that are known to proceed in good to high yields.[20,26,38,39] Compound **2·HH** shows good solubility in $CHCl_3$, CH_2Cl_2, toluene, Et_2O, and warm CH_3OH and is insoluble in H_2O. Furthermore, no appreciable amounts of phosphine oxidation/imine hydrolysis were observed when a $CDCl_3$ solution of **2·HH** was allowed to stand for 6 days.

The $^{31}P\{^1H\}$ NMR spectrum of **2·HH** in $CDCl_3$ displays a characteristic single resonance at δ(P) −10.0 ppm, and the expected imine CH═N resonance was observed in the ^1H NMR spectrum at δ(H) 8.97 ppm [^4J(PH) 3.6 Hz]. The CH_2N and OCH_2 protons appear as a doublet at 4.20 ppm and a singlet at 5.15 ppm, respectively. In the FT-IR spectrum the N(H) and CO stretches of the amide/carbamate functionalities are observed at 3332 and 1721, 1668 cm^{-1}, respectively. On the basis of a single-crystal X-ray structure analysis (vide infra) and previous literature examples, **2·HH** adopts the expected anti configuration.[20,26,38,50] Other characterizing data are given in the Experimental Section.

To evaluate whether **2·HH** is suitably preorganized for κ^4-PNN′N″-tetradentate coordination, an X-ray crystallographic study was undertaken. The molecular structure of **2·HH** (ORTEP view shown in Figure 1) clearly shows that condensation [C(7)−N(1) = 1.275(2) Å, Table 2] has resulted as borne out by the spectroscopic data previously discussed. Pyramidalization around P(1) is clearly reflected in the C−P−C bond angles, which lie in the range 102.24(7)−104.15(9)°. The N(2) hydrogen forms an asymmetric bifurcated weak intramolecular H-bond to both N(1) and N(3) [N(2)···N(1) 2.6414(18) Å, H(2)···N(1) 2.199(17) Å, N(2)−H(2)···N(1) 111.0(13)°; N(2)···N(3) 2.7533(18) Å, H(2)···N(3) 2.289(17) Å, N(2)−H(2)···N(3) 113.2(14)°]. Bifurcated interactions of this type have previously been observed by

(48) Antonaroli, S.; Crociani, B. *J. Organomet. Chem.* **1998**, *560*, 137−146.
(49) Ainscough, E. W.; Brodie, A. M.; Buckley, P. D.; Burrell, A. K.; Kennedy, S. M. F.; Waters, J. M. *J. Chem. Soc., Dalton Trans.* **2000**, 2663−2671.
(50) Banbery, H. J.; Hussain, W.; Hamor, T. A.; Jones, C. J.; McCleverty, J. A. *J. Chem. Soc., Dalton Trans.* **1990**, 657−661.

Table 2. Selected Bond Distances and Angles for Compounds **2·HH**, **3**, **4a**, **5a**·Et_2O, anti-**6a**·$CHCl_3$, syn-**6a′**·H_2O, anti-**6b**·$CHCl_3$, and anti-**6c**·CH_2Cl_2

	2·HH	**3** (M = Au)	**4a** (M = Pt)	**5a**·Et_2O (M = Pt)	anti-**6a**·$CHCl_3$ (M = Pt)	syn-**6a′**·H_2O (M = Pt)	anti-**6b**·HCl_3 (M = Pd)	anti-**6c**·H_2Cl_2 (M = Ni)
				Bond Length (Å)				
M(1)−P(1)		2.2397(17) [2.236(18)]	2.1977(5)	2.1845(11) [2.1818(12)]	2.2344(8)	2.2330(7)	2.2489(6)	2.1809(6)
M(1)−Cl(1)		2.2950(19) [2.292(2)]	2.2891(5)					
M(1)−Cl(2)			2.3921(5)					
M(1)−N(1)			2.0385(17)	2.088(3) [2.076(3)]	2.013(3)	2.015(2)	2.0191(19)	1.9070(17)
M(1)−C(36)				2.061(4) [2.070(4)]				
M(1)−N(2)				2.086(3) [2.096(3)]	2.004(3)	2.000(2)	1.9911(18)	1.8655(16)
M(1)−N(3)					1.995(3)	2.016(2)	1.9871(19)	1.8648(17)
C(7)−N(1)	1.275(2)	1.274(9) [1.256(9)]	1.286(3)	1.274(5) [1.280(5)]	1.291(4)	1.297(3)	1.289(3)	1.294(3)
N(2)−C(14)	1.3453(19)	1.344(8) [1.358(9)]	1.343(3)	1.335(5) [1.340(5)]	1.346(4)	1.341(3)	1.343(3)	1.345(3)
C(14)−O(1)	1.2292(17)	1.233(8) [1.230(8)]	1.221(3)	1.257(5) [1.246(5)]	1.242(4)	1.243(3)	1.241(3)	1.240(2)
N(3)−C(16)	1.350(2)	1.361(9) [1.348(9)]	1.345(3)	1.342(6) [1.348(6)]	1.348(4)	1.333(4)	1.336(3)	1.337(3)
C(16)−O(2)	1.2147(18)	1.199(9) [1.221(8)]	1.212(3)	1.198(6) [1.201(5)]	1.219(4)	1.238(3)	1.223(3)	1.225(3)
C(16)−O(3)	1.3530(17)	1.355(9) [1.342(0)]	[1.368(7)][a]	1.379(6) [1.371(6)]	1.367(4)	1.359(3)	1.377(3)	1.373(2)
				Bond Angle (°)				
Cl(1)−M(1)−P(1)		174.59(8) [175.47(9)	92.56(2)					
Cl(1)−M(1)−N(1)			178.94(5)					
Cl(1)−M(1) −Cl(2)			89.33(2)					
P(1)−M(1)−Cl(2)			177.58(2)					
N(1)−M(1)−Cl(2)			91.65(5)					
N(1)−M(1)−P(1)			86.47(5)	92.60(9) [92.18(10)]	95.53(8)	92.68(6)	95.43(5)	94.81(5)
C(36)−M(1)−P(1)				91.53(13) [90.12(13)]				
C(36)−M(1)−N(1)				173.7(2) [174.8(3)]				
C(36)−M(1)−N(2)				96.59(16) [98.23(15)]				
N(1)−M(1)−N(2)				79.37(12) [79.52(13)]	82.42(10)	82.32(9)	82.75(7)	84.61(7)
N(2)−M(1)−P(1)				171.86(9) [171.65(10)]	177.57(8)	174.51(7)	177.93(6)	178.45(5)
N(3)−M(1)−P(1)					100.79(8)	103.80(6)	100.54(6)	97.11(5)
N(1)−M(1)−N(3)					163.62(11)	163.52(9)	163.95(8)	167.98(7)
N(2)−M(1)−N(3)					81.23(11)	81.23(9)	81.25(8)	83.44(7)

[a] Weighted average for the two disorder components.

Bermejo[51] for an N_2O_2 tetradentate ligand. This arrangement clearly orientates all three nitrogen donor atoms toward each other, whereas the phosphorus center, with its associated lone pair, points away from the N_3 core. Rotation about the C(6)−C(7) bond would be anticipated to bring the P^{III} center into the same coordination environment as these three N donors. Furthermore, H(3) forms an intermolecular H-bond to O(1′) [N(3)···O(1′) 2.9254(17) Å, H(3)···O(1′) 2.114(19) Å, N(3)−H(3)···O(1′) 163.1(17)°. Symmetry operator: ′ = $x + 1$, y, z] leading to chains along the crystallographic a direction.

Attempts to cleave the N−CO_2Bz group with formation of the hybrid primary amine **2a** using 10% Pd on charcoal, cyclohexene in refluxing absolute EtOH (2 h) gave only unreacted **2·HH** (Scheme 1).[40,51] Oxidation of **2·HH** with aqueous H_2O_2 (27.5% w/w) in acetone followed by recrystallization from CH_2Cl_2/Et_2O/hexanes gave **2b** in 79% yield. The most informative evidence supporting **2b** came from the $^{31}P\{^1H\}$ NMR spectrum, which displayed a characteristic downfield shift [δ(P) 32.3 ppm]. This result suggests that the phosphorus lone pair on **2·HH** should be sufficiently basic to facilitate complexation and ultimately fulfill its function as a tetradentate ligand in combination with all three N donor centers.

Coordination Studies. Having successfully prepared **2·HH** we wished to explore its coordination chemistry with particular emphasis on probing possible ligating modes for this ligand. Our initial efforts focused on whether **2·HH** could behave as a κ^1-P-monodentate ligand like many other tertiary phosphines. Accordingly, when **2·HH** was reacted with AuCl(tht) in equimolar quantities, we isolated, as a yellow crystalline solid, the mononuclear compound AuCl-

(51) Bermejo, M. R.; González, A. M.; Fondo, M.; García-Deibe, A.; Maneiro, M.; Sanmartín, J.; Hoyos, V; Watkinson, O. L. *New J. Chem.* **2000**, *24*, 235−241.

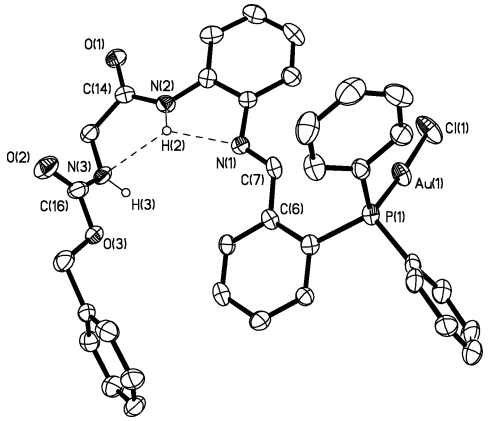

Figure 2. ORTEP plot of κ^1-P-monodentate **3** (one of the two, similar independent molecules is illustrated) showing the bifurcated intramolecular H-bonding. Thermal ellipsoids are drawn at the 50% probability level.

(**2·HH**), **3**, in high yield. The formulation of **3** was based on $^{31}P\{^1H\}$ [δ(P) 28.8 ppm], ^1H NMR studies (in dry CD_2Cl_2), and FT-IR which showed a ν_{AuCl} stretch at 330 cm^{-1}. However, when $^{31}P\{^1H\}$ NMR spectra of **3** are recorded in $CDCl_3$ two phosphorus-containing species are observed in roughly equal proportions. A resonance at δ(P) 29.0 ppm was confidently assigned to **3**, while that at δ(P) 32.2 ppm was ascribed to AuCl{2-$Ph_2PC_6H_4$(CHO)}, **I**,[52] presumably arising from hydrolysis of the CH═N imine bond of the coordinated **2·HH** ligand by trace amounts of water in $CDCl_3$. This is further corroborated by the ^1H NMR spectrum (in $CDCl_3$) which shows signals attributable to **I**, **3**, and the free amine **1**.

The X-ray structure of **3** has been determined (Figure 2, Table 2) and displays the expected near-linear geometry at the Au(I) metal center in both crystallographically independent molecules [174.59(8)° and 175.47(9)°]. The Au−Cl [2.2950(19) and 2.292(2) Å] and Au−P [2.2397(17) and 2.2361(18) Å] bond lengths for **3** are normal.[53] Reminiscent of **2·HH**, each independent molecule exhibits two weak intramolecular N−H···N H-bonds [N(2)···N(1) 2.641(8) Å, H(2)···N(1) 2.20 Å, N(2)−H(2)···N(1) 110° and N(2)···N(3) 2.720(8) Å, H(2)···N(3) 2.25 Å, N(2)−H(2)···N(3) 113° for molecule 1; N(5)···N(4) 2.646(8) Å, H(5)···N(4) 2.20 Å, N(5)−H(5)···N(4) 111° and N(5)···N(6) 2.747(8) Å, H(5)···N(6) 2.27 Å, N(5)−H(5)···N(6) 114° for molecule 2]. Additionally, each type of unique molecule forms a H-bonded chain along the *a* axis via weak N−H···O intermolecular H-bonds [N(3)···O(1)′ 2.860(7) Å, H(3)···O(1)′ 1.99 Å, N(3)−H(3)···O(1)′ 168° for molecule 1; N(6)···O(4)″ 2.868(8) Å, H(6)···O(4)″ 2.00 Å, N(6)−H(6)···O(4)″ 169° for molecule 2. Symmetry operator: ′ = $x - 1/2, -y, z$, ″ = $x - 1/2, -y + 1, z$].

Iminophosphines[24,54,55] are known to behave as κ^2-PN-ligands toward precious metal centers such as Pd^{II} and Pt^{II}. Furthermore, Klein[56] and Kurosawa[57] have independently shown this class of ligand can also undergo imine C−H bond activation. We find when **2·HH** is reacted with MCl_2(cod) (M = Pt, Pd) in CH_2Cl_2 the complexes MCl_2(**2·HH**) (M = Pt **4a**, M = Pd **4b**) are obtained in high yields (Scheme 2). Alternatively complex **4c** (92%) was readily prepared by reaction of 1 equiv of **2·HH** with Pd(CH_3)Cl(cod) in CH_2Cl_2. All three complexes displayed spectroscopic features consistent with κ^2-PN chelation. Hence, downfield ^{31}P chemical shifts are observed [δ(P) 4.2 for **4a**; 30.6 for **4b**; 36.9 ppm for **4c**] with respect to the free ligand **2·HH** [δ(P) −10.0 ppm]. Furthermore, in the case of **4c**, the ^1H NMR spectrum confirmed the presence of a single geometric

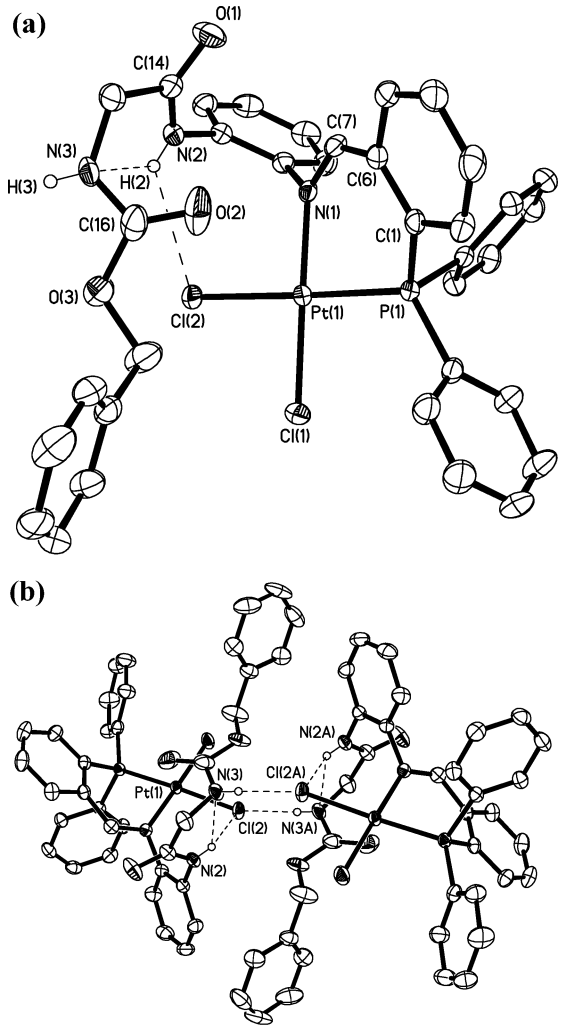

Figure 3. (a) ORTEP plot of κ^2-PN-didentate **4a** showing the bifurcated intramolecular H-bonding. Thermal ellipsoids are drawn at the 50% probability level. (b) ORTEP plot of **4a** showing the chairlike hydrogen-bonding arrangement (A = $-x, -y + 2, -z$). Thermal ellipsoids are drawn at the 50% probability level.

(52) Smith, M. B.; Elsegood, M. R. J.; Dale, S. H. *Acta. Crystallogr.* **2006**, *E62*, m1850−m1852.
(53) Smith, M. B.; Dale, S. H.; Coles, S. J.; Gelbrich, T.; Hursthouse, M. B.; Light, M. E. *CrystEngComm* **2006**, *8*, 140−149.
(54) (a) Crociani, B.; Antonaroli, S.; Marini, A.; Matteoli, U.; Scrivanti, A. *Dalton Trans.* **2006**, 2698−2705. (b) Crociani, B.; Antonaroli, S.; Canovese, L.; Uguagliati, P.; Visentin, F. *Eur. J. Inorg. Chem.* **2004**, 732−742. (c) Crociani, B.; Antonaroli, S.; Di, Vona, M. L.; Licoccia, S. *J. Organomet. Chem.* **2001**, *631*, 117−124. (d) Crociani, B.; Antonaroli, S.; Bandoli, G.; Canovese, L.; Visentin, F.; Uguagliati, P. *Organometallics* **1999**, *18*, 1137−1147.
(55) Ainscough, E. W.; Brodie, A. M.; Burrell, A. K.; Derwahl, A.; Jameson, G. B.; Taylor, S. K. *Polyhedron* **2004**, *23*, 1159−1168.
(56) Klein, H.-F.; Beck, R.; Flörke, U.; Haupt, H.-J. *Eur. J. Inorg. Chem.* **2002**, 3305−3312.
(57) Ohtaka, A.; Kato, N.; Kurosawa, H. *Organometallics* **2002**, *21*, 5464−5466.

Scheme 2. Preparation of Compounds **3**, **4a**−**c**, and **5a**, **5b**[a]

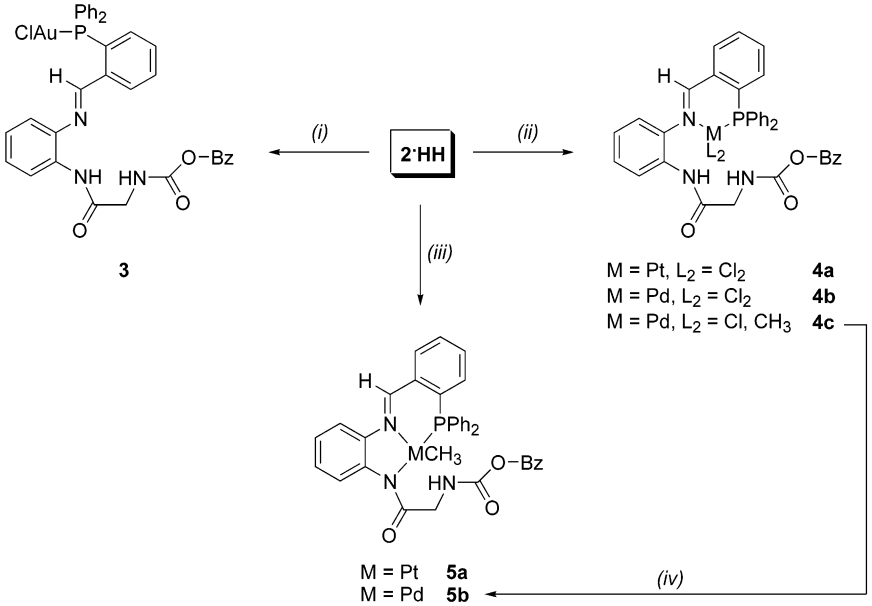

[a] Key: Reagents and conditions: (*i*) AuCl(tht), CH_2Cl_2 (*ii*) MCl_2(cod) or Pd(CH_3)Cl(cod), CH_2Cl_2 (*iii*) Pt(CH_3)$_2$(cod), CH_2Cl_2 (*iv*) ^{t}BuOK, CH_3OH.

isomer since only one Pd−CH_3 resonance [δ(H) 0.60 ppm, ^3J(HP) 3.1 Hz] was observed. We believe this geometric isomer to have the phosphine (−PPh_2) group trans to the chloride ligand as previously reported in related methylchloropalladium(II) complexes of P/N-chelating ligands.[58]

An X-ray crystallographic study of **4a** (Figure 3a, Table 2) was undertaken. The complex displays an approximate square-planar geometry around Pt(1) [86.47(5)−92.56(2)°] and comprises a six-membered P,N-chelate ring and two terminal chlorides. The difference in Pt−Cl bond lengths [2.2891(5) Å for Cl(1) trans to N(1); 2.3921(5) Å for Cl(2) trans to P(1)] is a result of the trans influence.[59] The $PtPC_3N$ six-membered ring is approximately hinged about a line from P(1) to the midpoint of the CH═N bond [mean plane of N(1)−Pt(1)−P(1) versus P(1)−C(1)−C(6)−C(7) = 50.4°]. The hydrogen H(2) forms weak intramolecular H-bonds to both N(3) [N(2)···N(3) 2.753(3) Å, H(2)···N(3) 2.40(3) Å, N(2)−H(2)···N(3) 111(2)°] and Cl(2) [N(2)···Cl(2) 3.263(2) Å, H(2)···Cl(2) 2.75(3) Å, N(2)−H(2)···Cl(2) 130(3)°]. This arrangement suggests how N(2)−H(2) amide deprotonation [coupled with HX (X = Cl, CH_3) elimination] may be accomplished, thus achieving a κ^3-PNN′ ligation mode for **2·H**$^-$. Molecules of **4a** form head-to-tail dimers (Figure 3b) in which each half is related by an inversion center through pairs of N(3)−H(3)···Cl(2A) interactions [N(3)···Cl(2A) 3.285(2) Å, H(3)···Cl(2A) 2.58(3) Å, N(3)−H(3)···Cl(2A) 159(3)°. Symmetry operator: A = $-x$, $-y + 2$, $-z$] resulting in an $R^4_4(8)$ chair-shaped H-bond motif.

In an effort to validate whether **2·HH** can function as a κ^3-PNN′-bonded ligand **2·H**$^-$ we selected Pt(CH_3)$_2$(cod) as a suitable precursor. This compound is not only susceptible to facile displacement of the labile cod ligand by PN-hybrid ligands but also reactive toward protonolysis[60] of one or both methyl ligands by suitable reagents. van Koten and co-workers[61] have shown that methylpalladium(II) alkoxides and aryloxides can be prepared from the corresponding dimethylpalladium(II) complexes and an appropriate alcohol (with elimination of CH_4). Furthermore Klein and co-workers[62] have shown that the aminophosphines 2-$Ph_2PC_6H_4N(H)R$ (R = H, CH_3) react with Co(CH_3){P(CH_3)$_3$}$_4$ to afford the pentacoordinate complex Co{κ^2-P,N-2-$Ph_2PC_6H_4NR$}{P(CH_3)$_3$}$_3$ with elimination of CH_4. Accordingly, reaction of Pt(CH_3)$_2$(cod) with 1 equiv of **2·HH** in toluene at room temperature gave Pt(CH_3)(**2·H**$^-$), **5a**, in excellent yield (81%) as an air-stable, yellow solid (Scheme 2). The analogous palladium(II) complex **5b** was obtained by treatment of **4c** with ^{t}BuOK in CH_3OH. The $^{31}P\{^1H\}$ NMR spectrum of **5a** showed a singlet, flanked by ^{195}Pt satellites, the difference in chemical shift and ^1J(PtP) coupling constant being approximately 10 ppm and 130 Hz, respectively, in comparison to the dichloroplatinum complex **4a**. Furthermore, the ^{1}H NMR spectrum clearly shows a Pt−CH_3 group [0.69 ppm, ^2J(HPt) 85.8 Hz], indicating retention of one methyl ligand within the coordination sphere of platinum and therefore one protonated amide nitrogen.

To confirm that N(2) has undergone platination we undertook an X-ray crystallographic study of **5a** (Figure 4a and b, Table 2). Like **4a**, the geometry around Pt in the two independent molecules is approximately square-planar [the coordination angles lie in the range 79.37(12)° for N(1)−Pt(1)−N(2) to 98.23(15)° for C(36)−Pt(1)−N(2)]. The Pt−P distances [2.1845(11) and 2.1818(12) Å for both independent

(58) (a) Durran, S. E.; Smith, M. B.; Dale, S. H.; Coles, S. J.; Hursthouse, M. B.; Light, M. E. *Inorg. Chim. Acta* **2006**, *359*, 2980−2988. (b) Chen, H.-P.; Liu, Y.-H.; Peng, S.-M.; Liu, S.-T. *Organometallics* **2003**, *22*, 4893−4899.

(59) (a) Housecroft, C. E.; Sharpe, A. G. *Inorganic Chemistry*; Pearson Educational: Harlow, England, 2001; p 574. (b) Greenwood, N. N.; Earnshaw, A. *Chemistry of the Elements*, 2nd ed.; Butterworth Heinemann, Oxford, 1997; pp 1164−1165.

(60) Romeo, R.; D'Amico, G. *Organometallics* **2006**, *25*, 3435−3446.

(61) Kapteijn, G. M.; Spee, M. P. R.; Grove, D. M.; Kooijman, H.; Spek, A. L.; van Koten, G. *Organometallics* **1996**, *15*, 1405−1413.

(62) Klein, H.-F.; Beck, R.; Flörke, U.; Haupt, H.-J. *Eur. J. Inorg. Chem.* **2003**, 240−248.

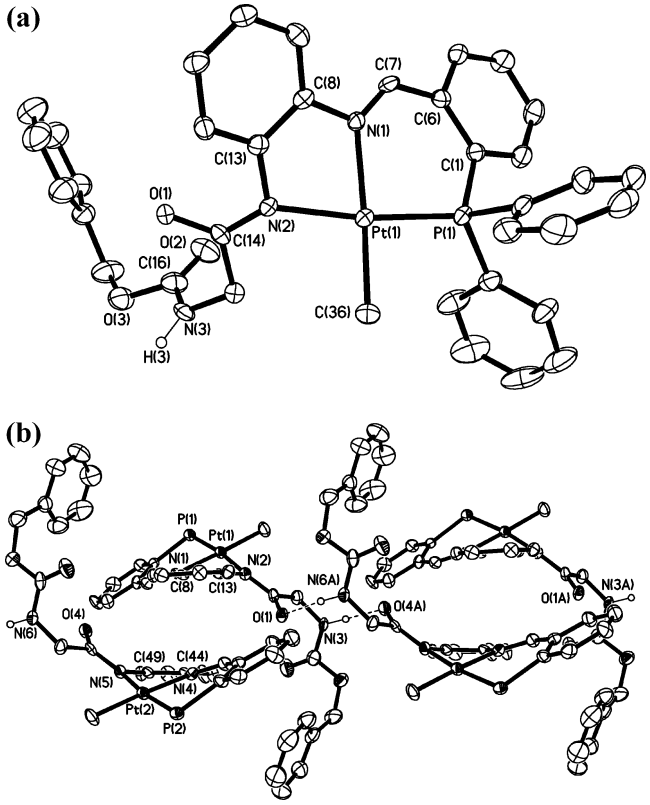

Figure 4. (a) ORTEP plot of complex **5a** showing the κ^3-PNN′ coordination mode (one of the two, similar independent molecules is illustrated). Thermal ellipsoids are drawn at the 50% probability level. (b) ORTEP plot of **5a** showing $\pi-\pi$ stacking and dimer pair formation through N−H···O intermolecular H-bonds. Symmetry operator: A = $x + 1$, y, z. Thermal ellipsoids are drawn at the 50% probability level. Phenyl groups on P(1) and P(2) omitted for clarity.

molecules] are shorter than those in **4a** [2.1977(5) Å], while the Pt−N(1) bond lengths are slightly different [2.088(3) and 2.076(3) Å for **5a**·Et_2O; 2.0385(17) Å for **4a**]. Similar to **4a**, the $PtPC_3N$ six-membered ring is approximately hinged about a line from P(1) to the midpoint of the CH═N bond [mean plane of N(1)−Pt(1)−P(1) versus P(1)−C(1)−C(6)−C(7) = 32.2°]. The reduction in this hinge angle (cf. 50.4° for **4a**) is presumably necessary to allow the formation of a PtN_2C_2 five-membered ring which itself is hinged about N(1)···N(2) [mean plane of N(1)−C(8)−C(13)−N(2) versus N(1)−Pt(1)−N(2) = 29.5°]. The two independent molecules of **5a** are related by approximate (noncrystallographic) inversion symmetry with groups N(1), N(2), C(8)>C(13) and N(4), N(5), C(44)>C(49) lying face-to-face in an inversion-related π-stacking arrangement (ca. 3.8 Å apart). In addition, these pairs are linked via two unique H-bonds [N···O 2.848-(5) and 2.842(5) Å, H···O 2.08 and 2.03 Å, N−H···O 146° and 152°] to neighboring pairs to give a chain along the *a* axis (Figure 4b).

During the course of this transformation we were intrigued to verify whether the platinum(II) intermediate $Pt(CH_3)_2$(**2·HH**) in which **2·HH** is initially κ^2-PN-didentate could be observed in solution prior to conversion to **5a**. Reaction of **2·HH** with $Pt(CH_3)_2$(cod) in C_6D_6 was monitored by $^{31}P\{^1H\}$ and ^1H NMR spectroscopy over ca. 2 h (after this time complex **5a** crystallizes from solution hampering any further NMR studies). A $^{31}P\{^1H\}$ NMR spectrum of a freshly prepared solution of $Pt(CH_3)_2$(cod)/**2·HH** revealed the following phosphorus compounds: **5a**, unreacted **2·HH** and two new species at δ(P) 21.3 [^1J(PtP) 1853 Hz] and 25.2 ppm [^1J(PtP) 1824 Hz] in an approximate ratio of 2.3:3:3.5:1, respectively. The similarity of both these phosphorus chemical shifts and ^1J(PtP) coupling constants [P trans to CH_3] suggest congruous structures which we cautiously assign to the conformational isomers **A** and **B** (alternate structures based upon slow rotation about the N(H)−CO_2Bz and/or C_{aryl}−N═C bonds cannot be discounted). Further support for the major conformational isomer at δ(P) 21.3 ppm comes from the ^1H NMR spectrum which shows characteristic, well-resolved resonances for the two inequivalent Pt−CH_3 ligands [δ(H) 1.45 ppm, ^2J(HPt) 86 Hz, ^3J(HP) 7.6 Hz; δ(H) 0.95 ppm, ^2J(HPt) 65 Hz, ^3J(HP) 5.2 Hz]. After ca. 20 min the concentration of **5a** increases as the intensity of the signal at δ(P) 21.3 ppm diminishes. After approximately 2 h, the predominant species present in solution is at δ(P) 25.2 ppm (in addition to some **5a**). Tentatively, we assign the resonance at δ(P) 21.3 ppm to **A** and that at δ(P) 25.2 ppm to **B**. We

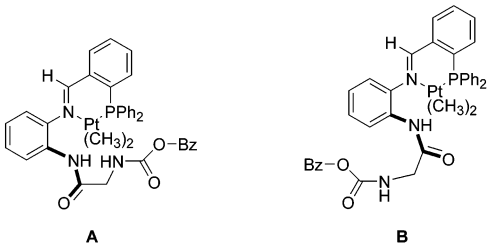

base this distinction on the assumption the observed orientation of the PtN−C(O) group in the final complex **5a** is that adopted in the intermediate **A**. Restricted rotation about this amide group is most likely to be important here and influenced by, among others, steric factors and/or hydrogen bonding.

Hedden and Roundhill[63] previously demonstrated that palladium(II) and platinum(II) complexes with the didentate ligand 2-$Ph_2PC_6H_4${CON(H)Ph}, when treated with base, afford the corresponding N-bonded amido complexes. To promote κ^4-PNN′N″ coordination of **2·HH** we treated **4a** (or **4b**) with slightly greater than 2 equiv of ^{t}BuOK in CH_3-OH and obtained very high yields of the unprecedented neutral compounds anti-**6a**\syn-**6a′** and anti-**6b**\syn-**6b′**, respectively (Scheme 3). In this procedure deprotonation of both N(H) protons would generate the corresponding diamide anion $\mathbf{2}^{2-}$, and concomitant five-membered chelate ring closure would lead to κ^4-PNN′N″ complexation. Alternatively, anti-**6b**\syn-**6b′** could be prepared successfully as a bright orange solid (93%), in one step, directly from Pd-$(OAc)_2$ and **2·HH** in CH_2Cl_2. In contrast, attempts to induce a second CH_4 elimination from **5a** under more forcing conditions (reflux, toluene, 19 h) failed to produce anti-**6a**\syn-**6a′**, indicating a lower reactivity of this N−H group toward methyl protonation. The corresponding nickel(II) complex anti-**6c**\syn-**6c′** was synthesized in 82% yield from $NiCl_2·6H_2O$, **2·HH**, and ^{t}BuOK in refluxing CH_3OH (1 h).

(63) Hedden, D.; Roundhill, D. M. *Inorg. Chem.* **1985**, *24*, 4152−4158.

Scheme 3. Preparation of **6a**−**c**′[a]

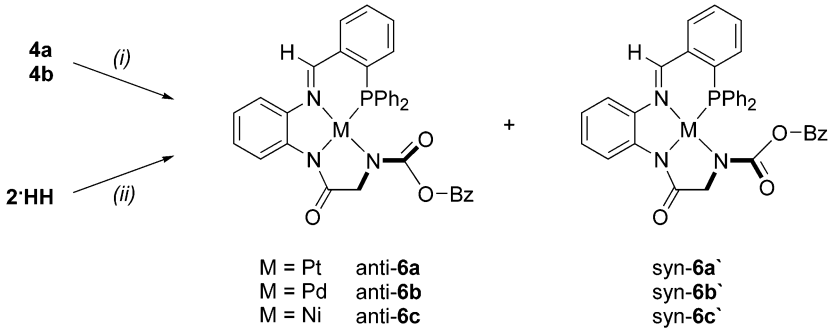

[a] Key: Reagents and conditions: (*i*) Excess ^{t}BuOK, CH_3OH (*ii*) $NiCl_2 \cdot 6H_2O$, ^{t}BuOK, CH_3OH.

The diamagnetic, square-planar red or orange complexes were characterized by NMR, IR, and X-ray crystallography.

The most interesting aspects regarding **6a**−**c** are the presence of two species in solution exhibiting very similar $^{31}P\{^1H\}$ and ^1H NMR properties. We attribute these species as the conformational isomers anti-**6a**\syn-**6a**′, anti-**6b**\syn-**6b**′, and anti-**6c**\syn-**6c**′, which we believe to result from restricted amide rotation (highlighted in bold lines as shown in Scheme 3).[64,65] To probe this further we carried out some variable-temperature NMR studies on anti-**6a**\syn-**6a**′ over high- and low-temperature regimes (see Supporting Information for these figures). At 295 K all the ^1H resonances show signs of line broadening, especially those in the aromatic and imine CH═N regions. On raising the temperature to 333 K (in $CDCl_3$) signals in the range 8.40−9.00 ppm sharpen to give a doublet at 8.87 ppm and a singlet at 8.82 ppm, flanked by ^{195}Pt satellites [^3J(HPt) 80 Hz]. In the region 3.80−5.00 ppm, a sharp singlet at 4.70 [^3J(HPt) 27.2 Hz] and a broad signal at 4.52 ppm was observed which should be compared with the four signals at 4.80, 4.70, 4.66, and 3.90 ppm when recorded at 295 K. These differences and those seen in the $^{31}P\{^1H\}$ NMR spectra (coalescence occurs at ca. 313 K) imply in the low-temperature regime, both anti-**6a** and syn-**6a**′ interconvert slowly on the NMR time scale. At higher temperatures interconversion between these conformational isomers is fast and a time-averaged spectrum results. These same features are also observed for the palladium(II) complexes anti-**6b**\syn-**6b**′. While common in amide chemistry, to the best of our knowledge this behavior has not previously been observed before with metal-coordinated unsymmetrical tetradentate-functionalized phosphines.

Furthermore, the IR spectra showed the absence of any NH vibrations in accord with deprotonation of both NH donor groups with new bands observed at ca. 1620 cm^{-1} typical of a carbonyl amide functional group (1630−1640 cm^{-1}).

The X-ray structure determinations of anti-**6a**·$CHCl_3$ (Figure 5a), syn-**6a**′·H_2O (Figure 5c), anti-**6b**·$CHCl_3$, and anti-**6c**·CH_2Cl_2 have each been performed with selected bond lengths and angles shown in Table 2. Complexes anti-**6a**·$CHCl_3$ and anti-**6b**·$CHCl_3$ are isostructural, while anti-**6c**·CH_2Cl_2 is indistinguishable from that of anti-**6a**·$CHCl_3$ and is not shown (see Supporting Information for these figures).

In all four structures the geometry around the metal(II) center is approximately square-planar with smallest bite angles in the range 81.23(9)−83.44(7)° [N(2)−M(1)−N(3)] and the largest angles of 97.11(5)−103.80(6)° [N(3)−M(1)−P(1)]. The M−P bond lengths [2.2344(8) (anti-**6a**), 2.2330(7) (syn-**6a**′), 2.2489(6) (anti-**6b**), and 2.1809(6) Å (anti-**6c**)] differ in the expected way on the basis of the metal radii. The Pd−P distance in anti-**6b** is very similar to that reported for a κ^1-P-monodentate phosphine-amide complex of palladium(II)[65] and the N(1)−Pd−P(1) angle [95.43(5)°] falls in the expected range.[66] Otherwise, there are very small differences in the M−N_{amide} bond lengths with respect to M−N_{imine} distances. To the best of our knowledge, only one other crystallographically characterized mononuclear complex with a PNN′N″ (−PPh_2, imine N, primary NH_2, and secondary NH) core has been reported.[39] The M(1) metal atom resides out of the basal plane of the P(1), N(1), N(2), and N(3) donor substituents by 0.0229 (anti-**6a**), 0.0159 (syn-**6a**′), 0.0215 (anti-**6b**), and 0.0246 Å (anti-**6c**). A major difference between **6a** and **6a**′ is the relative anti and syn conformation of the N−C(O)OBz functionality. In anti-**6a** the −OBz group lies away from the −PPh_2 substituent, but in syn-**6a**′ this situation is reversed. While there are no obvious differences in electron delocalization within the N(3)−C(16)−O(2) bond lengths, the two conformational isomers are distinguished by the orientation of C(16)═O(2) and N(3)−Pt(1). The two conformers anti-**6a** (Figure 5b) and syn-**6a**′ (Figure 5d) display similar geometries for the five- and six-membered rings. In anti-**6a**, the $PtPC_3N$ six-membered ring is approximately hinged about a line from P(1) to the midpoint of the CH═N bond [mean plane of N(1)−Pt(1)−P(1) versus P(1)−C(1)−C(6)−C(7) = 24.8°]. Within the PtN_2C_2 five-membered ring, the N(1)−C(8)−C(13)−N(2) portion is essentially planar (within ±0.03 Å) with Pt(1) being the flap of the envelope and 0.26 Å out of the N(1)−C(8)−C(13)−N(2) plane. In the second PtN_2C_2 five-membered ring, the N(2)−C(14)−C(15)−N(3) portion

(64) (a) Clayden, J.; Pink, J. H. *Angew. Chem., Int. Ed.* **1998**, *37*, 1937−1939. (b) Clayden, J.; Darbyshire, M.; Pink, J. H.; Westlund, N.; Wilson, F. X. *Tetrahedron Lett.* **1997**, *38*, 8587−8590.

(65) Sánchez, G.; García, J.; Meseguer, D.; Serrano, J. L.; García, L.; Pérez, J.; López, G. *Dalton. Trans.* **2003**, 4709−4717.

(66) Pérez, J.; Martínez, J. F.; García, L.; Pérez, E.; Serrano, J. L.; Sánchez, G. *Inorg. Chim. Acta* **2004,** *357*, 3588−3594.

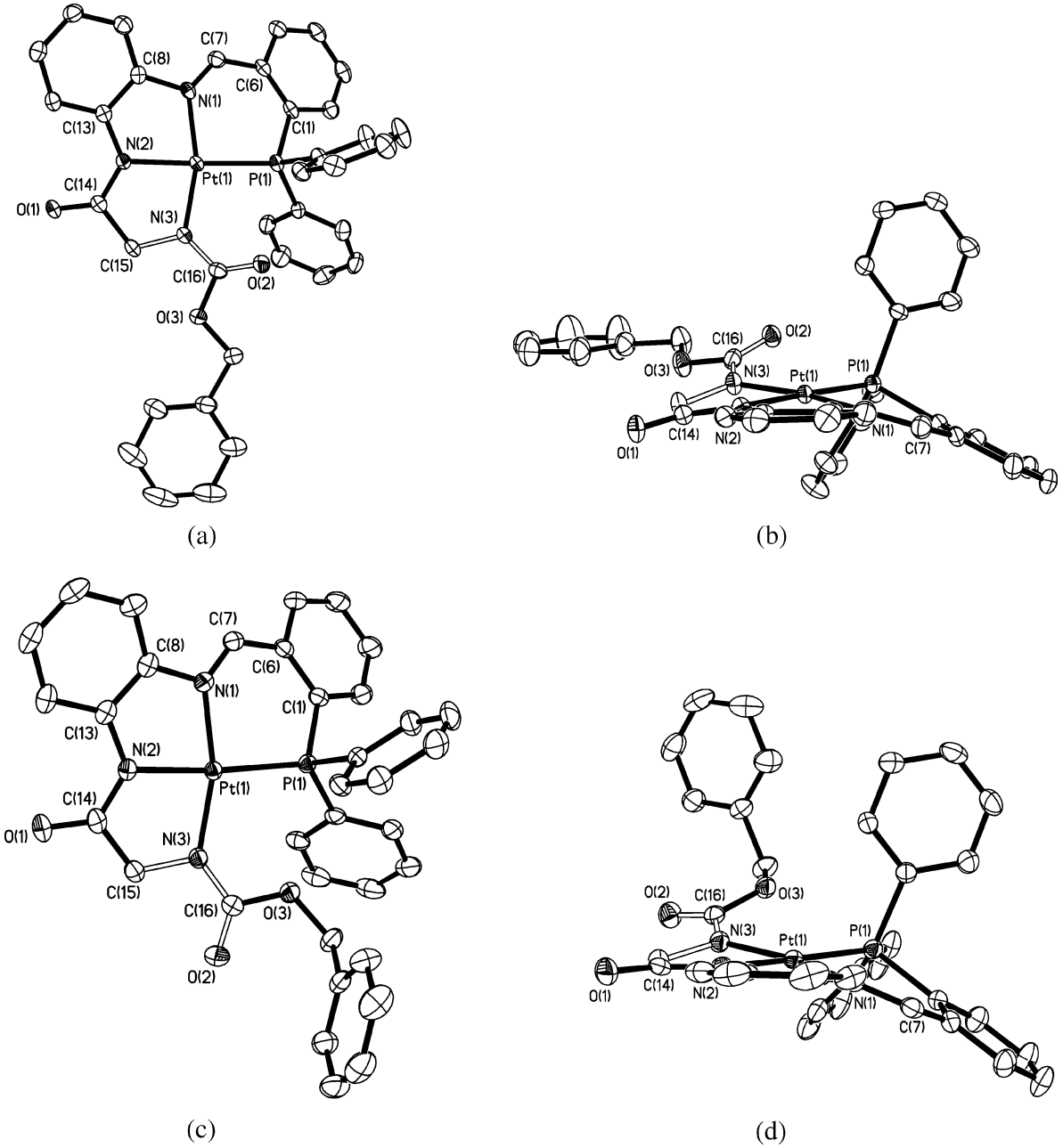

Figure 5. (a) ORTEP plot of κ^4-PNN′N″-tetradentate anti-**6a**. (b) Side projection of anti-**6a** showing the orientation of the N−C(O)OBz group and the metallocycle ring conformations. (c) ORTEP plot of κ^4-PNN′N′-′-tetradentate syn-**6a′**. (d) Side projection of syn-**6a′** showing the orientation of the N−C(O)-OBz group and the metallocycle ring conformations. All thermal ellipsoids are drawn at the 50% probability level.

is again more or less planar (within ±0.04 Å) with N(3) being the flap of the envelope and 0.30 Å out of the N(2)−C(14)−C(15)−N(3) plane. In the conformer syn-**6a′**, the $PtPC_3N$ six-membered ring is again approximately hinged about the vector that includes P(1) and the midpoint of the CH═N bond [mean plane of N(1)−Pt(1)−P(1) versus P(1)−C(1)−C(6)−C(7) = 30.4°]. The hinge angle is enlarged here by ca. 6° with respect to that observed for anti-**6a** yet approximately 20° less than seen in **4a**. Within the PtN_2C_2 five-membered ring, the N(1)−C(8)−C(13)−N(2) portion is coplanar to within ±0.03 Å with Pt(1) being the envelope flap lying 0.32 Å out of this plane. In the second PtN_2C_2 five-membered ring, the N(2)−C(14)−C(15)−N(3) portion is flat to within ±0.06 Å with C(15) being the flap of the envelope and 0.27 Å out of the N(2)−C(14)−C(15)−N(3) plane. In syn-**6a′**, molecules H-bond into pairs at an inversion center via pairs of bridging water molecules [O(4)···O(2′) 3.155(4) Å, H(4B)···O(2′) 2.17(4) Å, O(4)−H(4B)···O(2A) 145(3)°]; O(4)···O(1) 2.746(4) Å, H(4A)···O(1) 1.58(4) Å, O(4)−H(4A)···O(1) 177(3)°. Symmetry operator: ′ = $-x$, $-y$, $-z$].

Concluding Remarks

This work has demonstrated the versatile coordination behavior of a new tetradentate PNN′N″-ligand in which all three N centers are dissimilar. In light of all the spectroscopic and structural studies presented here, four different ligating modes (κ^1-P, κ^2-PN, κ^3-PNN′, κ^4-PNN′N″) have been

recognized for **2·HH** in its neutral (**2·HH**), monoanionic (**2·H**$^{-}$), and dianionic (**2**$^{2-}$) forms. In addition, the existence of both anti/syn conformational isomers in solution and the solid state has been observed. We are currently pursuing other types of tetradentate ligands with different donor-atom combinations and their coordination capabilities toward various metals. These results will be published in due course.

Acknowledgment. We should like to thank the EPSRC for funding (S.E.D.), Johnson and Matthey for the generous loan of precious metal salts and the EPSRC Mass Spectrometry Service Centre at Swansea. Dr Mark Edgar is gratefully acknowledged for acquiring the variable-temperature NMR spectra.

Supporting Information Available: Tables of crystal data and structure refinement, atomic coordinates, bond lengths and angles, anisotropic displacement parameters and hydrogen coordinates (CIF format) for **2·HH**, **3**, **4a**, **5a·**Et_2O, anti-**6a·**$CHCl_3$, syn-**6a′·**H_2O, anti-**6b·**$CHCl_3$, and anti-**6c·**CH_2Cl_2. Ellipsoid plots for anti-**6b·**$CHCl_3$ and anti-**6c·**CH_2Cl_2 along with VT NMR spectra [^{1}H, ^{31}P{^{1}H}] for anti-**6a**/syn-**6a′** are also included. This material is available free of charge via the Internet at http://pubs.acs.org.

IC061196S